BIOLOGY OF REPRODUCTION **84,** 715–722 (2011)
Published online before print 8 December 2010.
DOI 10.1095/biolreprod.110.088385

A Novel Role for Progesterone and Progesterone Receptor Membrane Component 1 in Regulating Spindle Microtubule Stability During Rat and Human Ovarian Cell Mitosis[1]

Valentina Lodde[3,4] and John J. Peluso[2,3]

Department of Cell Biology,[3] University of Connecticut Health Center, Farmington, Connecticut
Department of Animal Sciences,[4] University of Milan, Milan, Italy

ABSTRACT

The present studies were designed to assess the roles of progesterone (P4) and Progesterone Receptor Membrane Component 1 (PGRMC1) in regulating mitosis of spontaneously immortalized granulosa cells (SIGCs) and ovarian cancer cells, SKOV-3 cells. Because PGRMC1 has been detected among the proteins of the human mitotic spindle, we theorized that P4 and PGRMC1 could affect mitosis through a microtubule-dependent process. The present study confirms that SIGC growth is slowed by either P4 treatment or transfection of a PGRMC1 antibody. In both cases, slower cell proliferation was accompanied by an increased percentage of mitotic cells, which is consistent with a P4-induced prolongation of the M phase of the cell cycle. In addition, P4 increased the stability of the spindle microtubules, as assessed by the rate of beta-tubulin disassembly in response to cooling. Also, P4 increased spindle microtubule stability of SKOV-3 cells. This effect was mimicked by the depletion of PGRMC1 in these cells. Importantly, P4 did not increase the stability of the microtubules over that observed in PGRMC1-depleted SKOV-3 cells. Immunofluorescent analysis revealed that PGRMC1 is distributed to the spindle apparatus as well as to the centrosomes at metaphase. Further in situ proximity ligation assay revealed that PGRMC1 interacted with beta-tubulin. Taken together, these results suggest that P4 inhibits mitosis of ovarian cells by increasing the stability of the mitotic spindle. Moreover, P4's actions appear to be dependent on PGRMC1's function within the mitotic spindle.

centrosome, follicle, follicular development, granulosa cell, granulosa cells, mitosis, ovarian cancer cells, ovary, PGRMC1, progesterone/progesterone receptor, spindle

INTRODUCTION

Progesterone (P4) regulates female reproduction by influencing the function of several organs, including the hypothalamus [1, 2], the pituitary [1, 2], the mammary gland [3], and the uterus [3, 4]. Progesterone also has an intraovarian site of action where it influences different aspects of granulosa cell function, including those related to slowing the rate of granulosa cell mitosis and follicular growth (reviewed in Peluso [5] and Gellersen et al. [6]).

The effect of P4 on cell proliferation is cell type and dose dependent. Regarding the ovary, P4's inhibitory effect on granulosa cell proliferation has been observed both in vivo and in vitro [7–12]. In vitro, both nanomolar and micromolar concentrations of P4 inhibit proliferation of primary rat granulosa cells and spontaneously immortalized granulosa cells (SIGCs) [10]. In contrast, nanomolar concentrations of P4 stimulate proliferation of the ovarian surface epithelial cells as well as on ovarian cancer cell lines that are derived from these cells, whereas micromolar doses of P4 exert a marked antiproliferative effect on these cells [13, 14]. Thus, although P4 has dose-dependent effects depending on ovarian cell type, it is clear that micromolar P4 inhibits proliferation of cells derived from either primary granulosa cells or ovarian cancers. Importantly, the growth inhibitory effects of P4 that are observed at micromolar concentrations are physiologically relevant because follicular fluid concentrations of P4 in the rat ovary vary from a low of about 4 μM on diestrus I to a high of ≈57 μM on proestrus [15].

Despite its biological relevance, little is known about the mechanisms that are involved in regulating P4's antiproliferative activity in ovarian cells. A possible mediator of P4's action is Progesterone Receptor Membrane Component 1 (PGRMC1). Several lines of evidence support this hypothesis. Specifically, PGRMC1-depleted ovarian cancer cells (SKOV-3) [16], A549 non-small cell lung cancer cells [17], and MDA-MB-468 breast cancer cells [17] all grow slower in vitro than their parental cells. Finally, tumors derived from ovarian and breast cancer cells in which PGRMC1 expression was depleted by stable expression of short hairpin RNA grow slower than tumors derived from their respective parental cell lines [16, 17].

Progesterone's ability to inhibit the complex events involved in mitosis likely involves the regulation of numerous signal transduction pathways. Clearly, some of these P4-regulated pathways could involve PGRMC1. One possible site of PGRMC1's action is the mitotic spindle, because a phosphoproteome analysis detected PGRMC1 among the proteins of HeLa cell spindle extract [18]. Based on these observations, the present studies were designed to test the hypothesis that P4 and PGRMC1 slow the rate of ovarian cell mitosis, in part through a direct effect on the mitotic spindle.

MATERIALS AND METHODS

Cell Lines and Culture

All of the chemicals used in this study were purchased from Sigma Chemical Co. (St. Louis, MO), except for those specifically mentioned. The SIGCs (provided by Dr. Robert Burghardt, Texas A&M University, College Station, TX) were derived from rat granulosa cells isolated from preovulatory follicles as described by Stein et al. [19]. The human ovarian epithelial cancer cell line, SKOV-3, was obtained from the American Type Culture Collection (Manassas, VA). The PGRMC1-depleted SKOV-3 cell line (dsRed SKOV-3 PGRMC1 depleted) was obtained by stable expression of interfering short hairpin RNA in dsRed-expressing SKOV-3 cell line (dsRed SKOV-3), as described elsewhere [16].

Except where noted, cells were cultured in growth medium, which was Dulbecco modified Eagle medium/F12 supplemented with 5% of fetal bovine

[1]Supported by National Institutes of Health grant 5R01HD052740.
[2]Correspondence: John J. Peluso, Department of Cell Biology, University of Connecticut Health Center, 263 Farmington Avenue, Farmington, CT 06030. FAX: 860 679 1269; e-mail: peluso@nso2.uchc.edu

Received: 2 September 2010.
First decision: 27 September 2010.
Accepted: 30 November 2010.

eISSN: 1529-7268 http://www.biolreprod.org
ISSN: 0006-3363

serum (FBS; HyClone, Logan, UT), 100 U/ml penicillin G, and 100 μg/ml streptomycin, as previously described [10, 16]. When the effect of P4 on cell proliferation and spindle microtubule stability was evaluated (see below), the culture medium was supplemented with 5% of charcoal/dextran-treated FBS with reduced steroid levels (Hyclone). The dsRed-expressing SKOV-3 cells were maintained in growth medium supplemented with 100 μg/ml geneticin (GIBCO-Invitrogen, Grand Island, NY).

Unless otherwise indicated, a total of 4×10^5 cells were plated in 2 ml of medium in either 35-mm culture dishes (Greiner Bio-One GmbH, Frickenhausen, Germany), glass-bottom culture dishes (Mat Tek Corp., Ashland, MA), or on cover glasses in 35-mm culture dishes. Regardless of culture vessel, the cells were incubated for 24 h at 37°C with 5% CO_2 in a humidified atmosphere and then fixed for immunofluorescent staining or treated according to the experimental design. For Western blot analysis, a total of 4×10^6 cells were plated in 100-mm cell culture dishes and cultured for 24 h as described above prior to cell harvesting.

Immunodetection of PGRMC1

Western blot analysis. PGRMC1 was detected in whole-cell lysates obtained from SIGCs, dsRed SKOV-3, and dsRed SKOV-3 PGRMC1-depleted cells by Western blot analysis as previously described [16, 20]. Cells were lysed in RIPA buffer (50 mM Tris-HCl [pH 7.4], 150 mM NaCl, 1 mM ethylenediaminetetraacetic acid, and 1% Nonidet P-40, 0.25% Na deoxycolate), supplemented with protease and phosphatase inhibitors as previously described [20]. All procedures were conducted on ice. Total amount of protein was determined using the BCA assay kit from Pierce Biotechnology (Rockford, IL), and 10 μg of total protein was used for Western blot analysis. PGRMC1 immunodetection was conducted using a rabbit polyclonal antibody raised against amino acids 1–46 mapping at the N-terminus of PGRMC1 of human origin (catalogue no. sc-98680; Santa Cruz Biotechnology, Santa Cruz, CA) at a dilution of 1:200. PGRMC1 was revealed using an anti-rabbit horseradish peroxidase-labeled antibody (1:2000) and ECL detection (GE Healthcare, Chalfont St. Giles, U.K.). Negative controls were conducted by omitting the primary antibody. When PGRMC1 expression analysis was conducted on dsRed SKOV-3 and dsRed SKOV-3 PGRMC1-depleted cells, the nitrocellulose membrane was stripped in stripping buffer (100 mM 2-mercaptoethanol, 2% SDS, and 62.5 mM Tris-HCl [pH 6.7]) at 50°C for 30 min and reprobed with a GAPDH polyclonal antibody (catalogue no. AM4300; Ambion Inc., Austin, TX) at dilution 1:4000. This was done to confirm that equal amounts of total protein were loaded during the procedure. This served also as a control for the specificity of the anti-PGRMC1 antibody used in this study.

Immunofluorescence. Double immunofluorescent staining was conducted to colocalize PGRMC1 with either β-tubulin or γ-tubulin in 4% paraformaldehyde-fixed SKOV-3 cells. After fixation, cells were permeabilized with 0.1% Triton X-100 in PBS for 7 min and blocked with 3% bovine serum albumin in PBS for 1 h.

For the colocalization study of PGRMC1 and γ-tubulin, the samples were incubated overnight at 4°C with a solution of rabbit polyclonal anti-PGRMC1 antibody (1:500; catalogue no. sc-98680; Santa Cruz Biotechnology) and mouse monoclonal anti-γ-tubulin antibody (1:1000; clone GTU-88; catalogue no. T5326; Sigma-Aldrich, St. Louis, MO). Primary antibodies were detected with Alexa Fluor 546-labeled anti-rabbit and Alexa Fluor 488-labeled anti-mouse antibodies (Molecular Probes, Eugene, OR), respectively. For the colocalization study of PGRMC1 and β-tubulin, primary and secondary antibodies were incubated sequentially. β-Tubulin was immunodetected by using a mouse monoclonal anti-β-tubulin antibody (1:400; clone TUB 2.1; catalogue no. T4026; Sigma-Aldrich). All primary and secondary antibodies were diluted in 4% FBS in PBS. As negative controls, normal rabbit and/or mouse immunoglobulin G (IgG; Santa Cruz Biotechnology) were used in place of the primary antibodies. After DNA counterstaining with Hoechst 33342, samples were mounted on slides with ProLong antifade reagent (Invitrogen-Molecular Probes) and analyzed on a Zeiss Axio Observer inverted microscope (Carl Zeiss MicroImaging Inc., Thornwood, NY) equipped with both a Lumen 200 Fluorescence Illumination Systems (Prior Scientific Inc., Rockland, MA) and a QImaging Retiga EXi CCD digital camera (QImaging, Surrey, BC). Immunofluorescence was performed to assess the possible role of P4 in perturbing PGRMC1 localization on the spindle apparatus. To this purpose, cells were incubated for 7 min, 24 h, 48 h, and 72 h with either vehicle or 4 μM P4 and then processed as described above.

PGRMC1 immunostaining was also performed on both dsRed SKOV-3 and dsRed SKOV-3 PGRMC1-depleted cells as described above, with the exception that the secondary antibody was Alexa Fluor 488-labeled goat anti-rabbit. Images were captured under identical exposure times and gain settings. The total fluorescence intensity (FI) of the PGRMC1 staining in the spindle of metaphase cells was determined with the iVision-Mac Image Acquisition and Analysis Software (BioVision Technologies, Exton, PA) using the Hoechst-stained metaphase plate to identify the presumptive area of the spindle. In addition, the background FI was estimated by determining the average of the FI of the presumptive spindle areas in the IgG control group. Specific PGRMC1 FI was calculated by subtracting the background FI from the total PGRMC1 FI.

Antibody-Mediated Interference with PGRMC1 Function

In order to perturb PGRMC1 function in SIGCs, the anti-PGRMC1 antibody was delivered into the cells using the Chariot transfection reagent (Active Motif, Carlsbad, CA) as previously described [21]. This technology has successfully been applied to delivering antibodies into cells while preserving their ability to recognize their target antigens [22]. To demonstrate the feasibility and effectiveness of this approach, a total of 2×10^5 SIGCs were plated in glass-bottom culture dishes and cultured for 48 h prior to being transfected. Briefly, 12 μg of Chariot transfection agent was diluted in water and incubated for 30 min at room temperature with either PBS or 5 μg of Alexa Fluor 488-labeled IgG in PBS. Transfection was carried out by incubating SIGCs with the above mixture for 1 h at 37°C in serum-free Optimem (GIBCO-Invitrogen), according to the manufacturer's instructions. Thereafter, complete growth medium was added without removing the transfection mixture, and the cells were incubated for additional 2 h before being washed and observed under fluorescent microscopy to assess transfection efficiency. Alexa 488-IgG was not incorporated into the SIGCs unless the transfection agent was present. Moreover, in the presence of the transfection agent, transfection efficiency was estimated to be nearly 100%, confirming our previous study [21] (Supplemental Fig. S1, available online at www.biolreprod.org).

Having established that this protocol was highly effective in transfecting the SIGCs, it was used to deliver either the anti-PGRMC1 antibody or normal rabbit IgG into SIGCs. After transfection, the medium was replaced with growth medium, and cells were treated according to the experimental design to assess the effect on cell proliferation.

Cell Proliferation and Mitotic Index Assays

In order to assess the effect of P4 treatment on SIGC proliferation, cells were plated in growth medium supplemented with 5% charcoal/dextran-treated FBS, into 35-mm culture dishes to which a horizontal and two vertical axes were scribed on the bottom outer surface. After 3 h, cells were washed to remove any unattached cells and the cells cultured in growth medium with or without (CTRL) 4 μM P4. In the CTRL group, an equivalent amount of ethanol that was used to dissolve P4 was added. Bright-field images of the eight areas that were formed at the intersection of the horizontal and each vertical axis were taken. After 24 and 48 h of culture, images of the same eight areas were taken. The total number of cells present in each area was counted either manually or using the iVision-Mac Image Acquisition and Analysis Software. Cell proliferation was expressed as the fold increase in cell number over the Time 3 h value. In addition, the number of mitotic cells was recorded and expressed as a percentage of the total number of cells (mitotic index).

In order to assess the effect of perturbing PGRMC1 on SIGC proliferation, cells were transfected with either IgG or the anti-PGRMC1 antibody as described above. After 3 h of transfection, the medium was replaced with growth medium and cultured for an additional 21 h. In this experiment, pictures were taken from the same field of view at 3 and 21 h after transfection. The fold increase in cell number was calculated as described above. In order to calculate the mitotic index, cells were fixed in stabilization buffer (0.1 M PIPES [pH 6.75]; 1 mM ethylene glycol tetraacetic acid; 1 mM $MgSO_4$; 4% polyethylene glycol 6000; 1% Triton X; and 2% formaldehyde) for 10 min at 37°C, postfixed in methanol for 5 min at −20°C, and immunostained for β-tubulin as described above. Cells were analyzed under fluorescent microscopy. For each treatment, 10–15 fields were randomly selected, and the number of cells in metaphase, anaphase, telophase, and cytokinesis was recorded. The total number of cells was counted in each field, and the mitotic index was calculated as described above. An average of 400-1000 cells were counted for each treatment in each replicate.

In Vivo Disassembly/Reassembly of Spindle Microtubules

After various treatments, the cells were fixed either 1) immediately or 2) after incubation on ice for up to 60 min or 3) after incubation on ice for 60 min and rewarming by replacing the medium with warm medium and incubating for an additional 7 min at 37°C. As outlined in each experiment, cells were fixed in 100% methanol for 7 min at −20°C and then immunostained for β-tubulin to reveal the spindle as described above, with the exception that the incubation with the β-tubulin antibody was performed overnight at 4°C. Samples were analyzed under fluorescent microscopy, and images of randomly selected

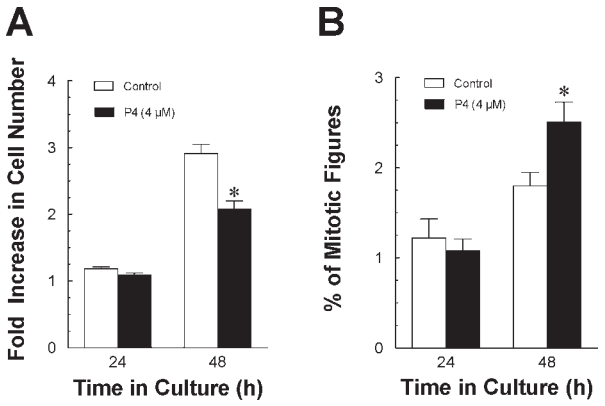

FIG. 1. The effect of P4 treatment on the fold increase in cell number (**A**) and the percentage of mitotic figures (**B**) in SIGCs after 24 and 48 h of culture. The fold increase in cell number and the mitotic index were assessed as outlined in *Materials and Methods*. Values are means ± SEM. *Significantly different value from the appropriate control value ($P < 0.05$).

metaphase cells were captured under identical exposure time and gain settings. The total FI of the β-tubulin staining in the spindle of 20–40 cells for each time point was determined with the iVision-Mac Image Acquisition Analysis Software and used as an indicator of the quantity of polymerized tubulin in each spindle. For each replicate, the mean FI of the β-tubulin staining calculated in the Time 0 group was set as 100%, and the mean FI values of other time points were expressed as a percentage of the Time 0 value.

In Situ Proximity Ligation Assay

The interaction between PGRMC1 and either β-tubulin or γ-tubulin was assessed by using the in situ Proximity Ligation Assay (PLA; Duolink II; OLINK Bioscience, Uppsala, Sweden) in SKOV-3 cells. This technology allows for detection of protein-protein interaction in fixed cells using a pair of oligonucleotide-labeled secondary antibodies (PLA probes), which generate a signal only when the two probes have bound in close proximity (http://www.olink.com/). The signal from each detected pair of PLA probes is visualized as an individual fluorescent spot. Duolink in situ PLA was performed as recommended by the manufacturer, with the exception that primary and secondary PLA probes were incubated sequentially. Samples were prepared as described above for immunofluorescence. Primary antibodies used were the mouse anti-β-tubulin, rabbit anti-α-tubulin (catalogue no. 2125; Cell Signaling Technology, Danvers, MA) as a positive control, and the indicated primary antibody pairs. The PLA probes used were the anti-rabbit PLUS and the anti-mouse MINUS. Negative control was performed omitting one of the two primary antibodies. In situ PLA was also performed to assess the possible role of P4 in perturbing PGRMC1-β-tubulin interaction. To this purpose, cells were incubated for 7 min with ether vehicle or 4 μM P4 and then processed as described above.

Statistical Analysis

All experiments were repeated two to four times, and data are presented as the mean ± SEM. Statistical significance was determined by Student unpaired *t*-test when means of two different groups were being compared. Means from three or more groups were compared using an ANOVA followed by a Tukey multiple-comparison test. Regardless of the statistical test, P values of <0.05 were considered significant.

RESULTS

As shown in Figure 1A, P4 treatment suppressed the serum-induced increase in SIGC number after 48 h of culture in growth medium ($P < 0.05$) compared with the control group. This was accompanied by a significant increase in the percentage of mitotic cells ($P < 0.05$; Fig. 1B). The P4-induced increase in the percentage of mitotic figures indicates that P4 prolongs the duration of the mitotic phase of the cell cycle.

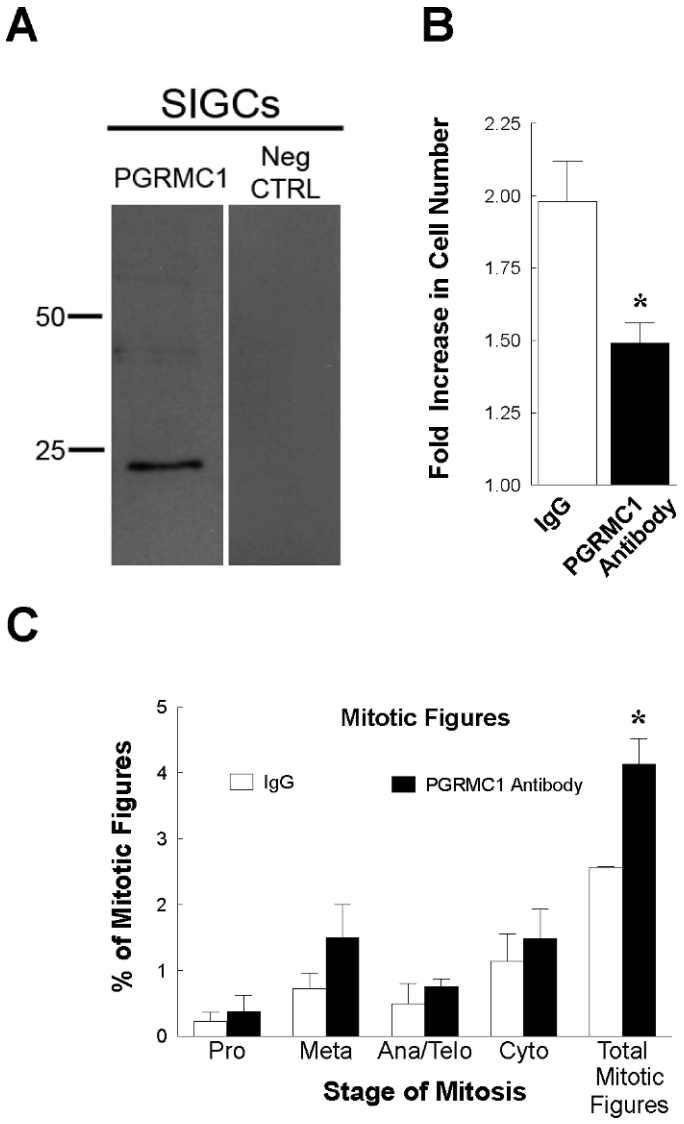

FIG. 2. Immunodetection of PGRMC1 in SIGCs by Western blot analysis using the rabbit polyclonal anti-PGRMC1 antibody (**A**); values in kDa. The effect of the presence of the anti-PGRMC1 antibody or IgG on the fold increase in cell number (**B**) and the percentage of mitotic figures (**C**) in SIGCs after 21 h of culture. The fold increase in cell number and the percentage of mitotic figures were assessed as outlined in *Materials and Methods*. Values are means ± SEM. *Significantly different value from the appropriate control value ($P < 0.05$). Pro, prophase; Meta, metaphase; Ana, anaphase; Telo, telophase; Cyto, cytokinesis.

Because P4 could be mediating its action through PGRMC1, we assessed the extent to which blocking the function of PGRMC1 with an antibody could affect the fold increase in cell number and the mitotic index. Spontaneously immortalized granulosa cells were transfected with either IgG or PGRMC1 antibody. As shown in Figure 2A, the PGRMC1 antibody used specifically recognized PGRMC1 in SIGCs, as revealed by Western blot analysis. When this antibody was transfected into SIGCs, the fold increase in cell number was reduced compared with the IgG control group ($P < 0.05$; Fig. 2B). In addition, the mitotic index (percentage of mitotic figures) was increased by PGRMC1 antibody treatment ($P < 0.05$; Fig. 2C).

Progesterone could influence the duration of mitosis by altering the rate of spindle microtubule disassembly and reassembly. To test this, the rate of disassembly and

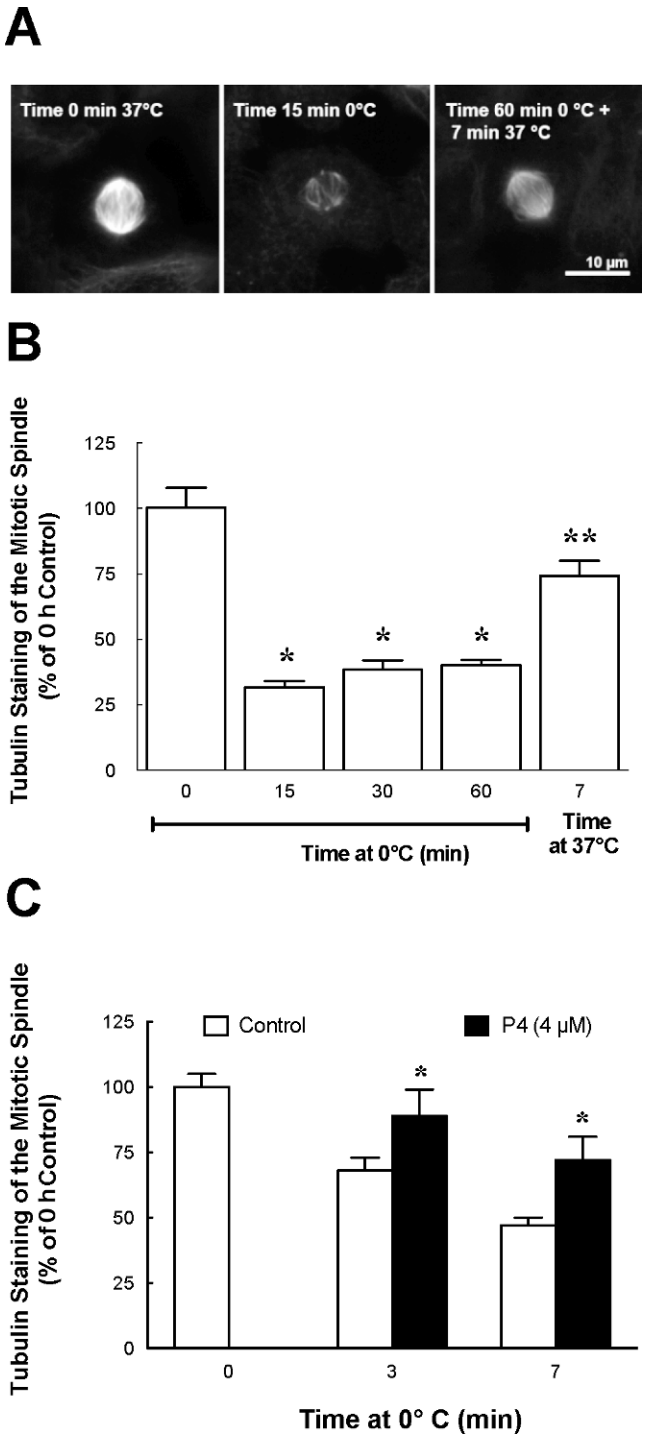

FIG. 3. Validation of the assay to assess the process of spindle microtubule disassembly and reassembly in response to cold treatment and rewarming. **A**) Representative fluorescent images of β-tubulin-immunostained metaphase SIGCs at Time 0, and after 15–60 min of incubation on ice or 7 min of rewarming. **B**) The mean ± SEM total FI of the β-tubulin staining in the spindle is shown as an indicator of the quantity of polymerized tubulin in each spindle. The mean FI of the β-tubulin staining calculated in the Time 0 group was set as 100%, and the mean FI values for the other time points were expressed as a percentage of the Time 0 value. **C**) Effect of P4 treatment on the process of spindle microtubules disassembly after 3 and 7 min of cooling. Values are means ± SEMs. *Significantly different value from the Time 0 control value ($P < 0.05$). **Significantly less than the Time 0 control value but greater than all other groups ($P < 0.05$).

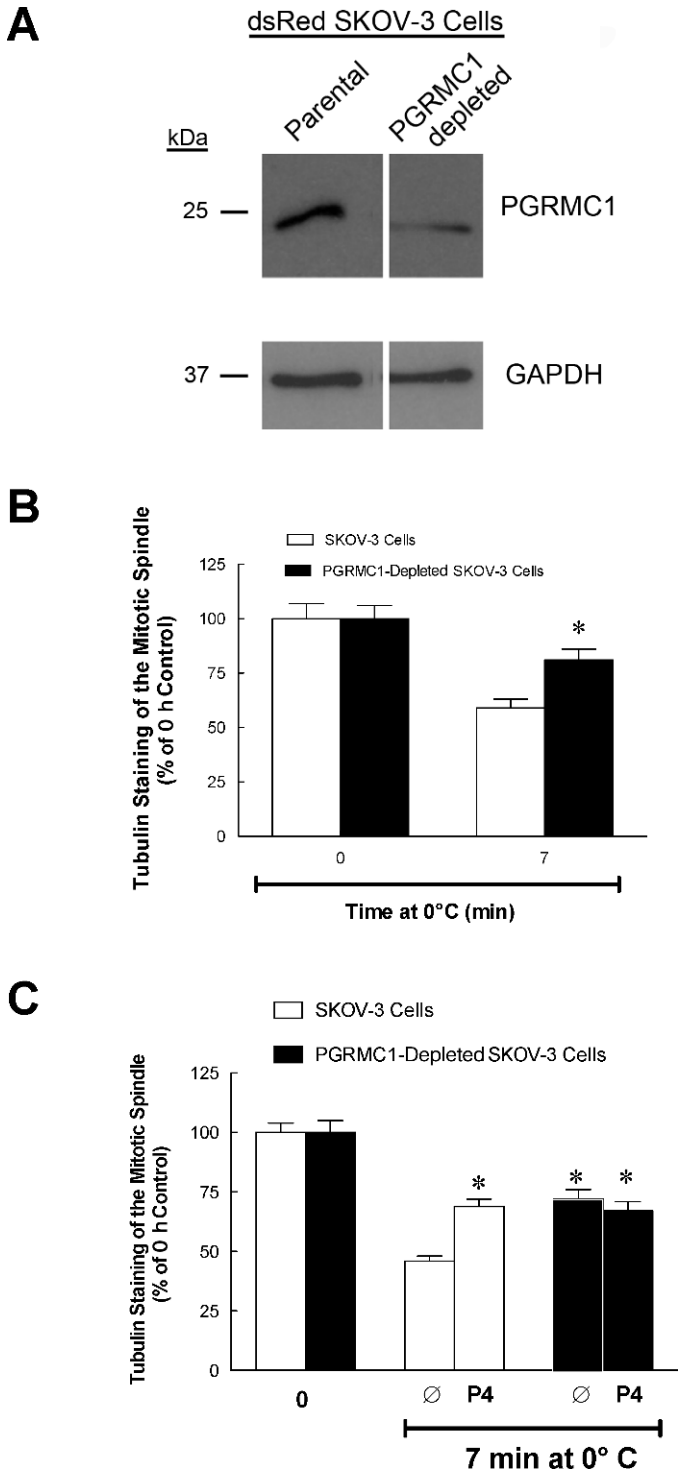

FIG. 4. Immunodetection of PGRMC1 expression by Western blot analysis in dsRed SKOV-3 parental and PGRMC1-depleted dsRed SKOV-3 cells. **A**) GAPDH Western blot is shown to demonstrate equal protein loading. **B**) The effect of PGRMC1 depletion in dsRed SKOV-3 cells on the process of disassembly of the spindle microtubules after 7 min of incubation on ice. **C**) The effect of P4 treatment on spindle microtubule disassembly after 7 min of incubation on ice in the parental and PGRMC1-depleted dsRed SKOV-3 cells. Values are means ± SEMs. *Significantly different value from the appropriate control value ($P < 0.05$).

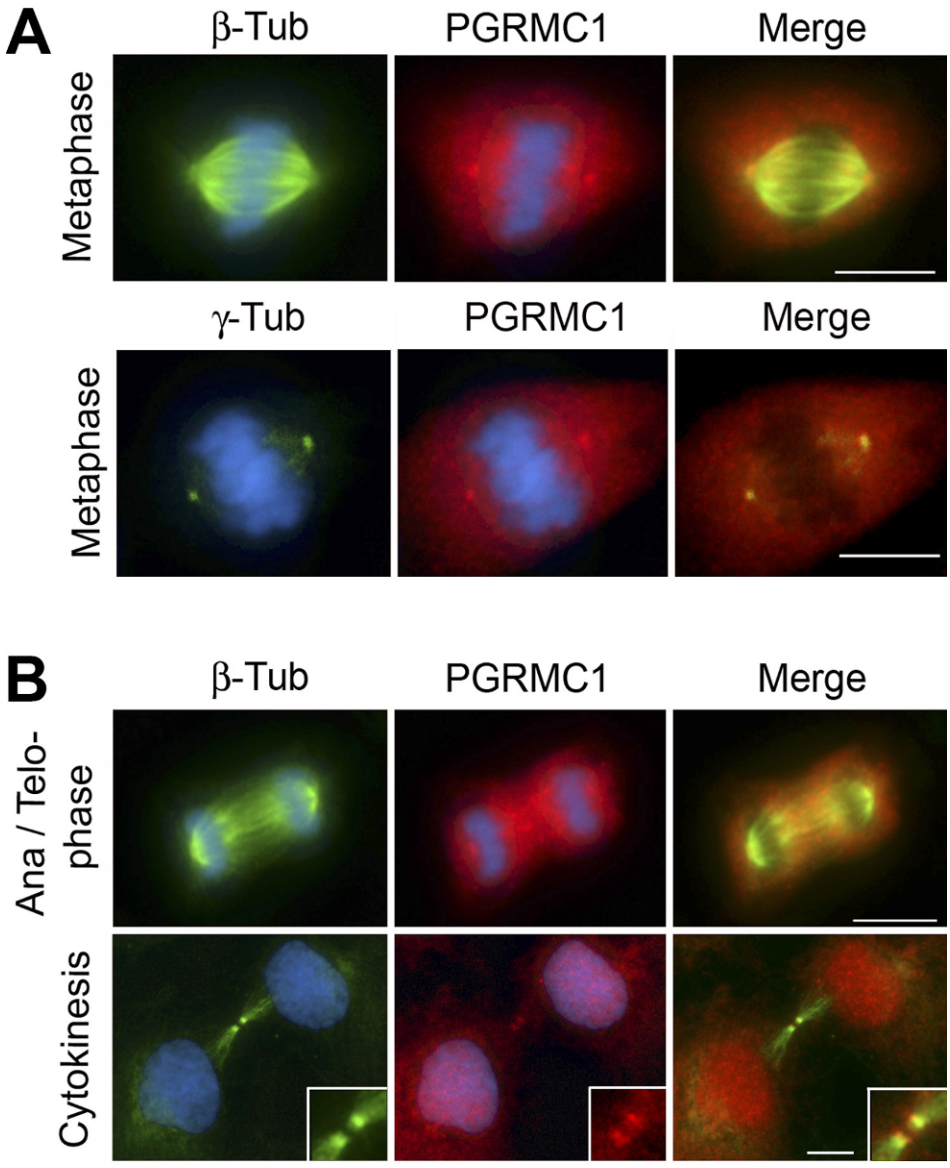

FIG. 5. **A**) Representative images showing coimmunostaining of PGRMC1 (red) and β-tubulin (β-Tub) or γ-tubulin (γ-Tub; green) at metaphase in SKOV-3 cells. **B**) Representative images showing coimmunostaining of PGRMC1 and β-tubulin at anaphase/telophase and cytokinesis in SKOV-3 cells. DNA is counterstained with Hoechst 33342 (blue). The PGRMC1 and β-tubulin or PGRMC1 and γ-tubulin merged images are shown in the left panels. In **B** (lower row), the inset represents a 3× magnification of the midbody. Bar = 10 μm.

reassembly was estimated by sequentially exposing SIGCs to cold treatment to induce disassembly, and rewarming to stimulate reassembly [23, 24]. As shown in Figure 3, A and B, the FI of the mitotic spindle decreased to approximately 30% of its initial value ($P < 0.05$) after 15 min of cooling and remained at this level for up to 60 min. After 7 min at 37°C, the metaphase spindle reassembled to 75% of the initial FI. The presence of P4 during the cooling procedure slowed down the rate of microtubule disassembly after 3 and 7 min of incubation on ice ($P < 0.05$; Fig. 3C). Progesterone was not effective in inhibiting microtubule disassembly after 60 min of cooling and did not affect the process of reassembly after rewarming (data not shown). These data indicate that P4 increases the stability of the spindle microtubules in response to cooling.

Because the presence of the antibody makes it technically difficult to more clearly define the relationship between P4, PGRMC1, and mitotic spindle stability, subsequent studies were designed to assess PGRMC1's role in regulating spindle stability by comparing the effect of P4 on parental dsRed SKOV-3 and PGRMC1-depleted dsRed SKOV-3 cells. That PGRMC1 was effectively reduced in the PGRMC1-depleted dsRed SKOV-3 cells was confirmed by Western blot analysis (Fig. 4A). Interestingly, depleting PGRMC1 in dsRed SKOV-3 cells significantly slowed the rate of the spindle microtubule disassembly after 7 min of incubation on ice ($P < 0.05$; Fig. 4B). As observed for SIGCs, treating dsRed SKOV-3 cells with P4 slowed the rate of microtubule disassembly in response to cooling compared with the control group ($P < 0.05$; Fig. 4C). PGRMC1 depletion also slowed that rate of disassembly, mimicking the effect of P4 seen in the parental dsRed SKOV-3. Further, the rate of spindle microtubule disassembly in the PGRMC1-depleted cells dsRed SKOV-3 was not influenced by the presence of P4 (Fig. 4C).

Because PGRMC1 influences spindle microtubule stability, its presence on the mitotic spindle of SKOV-3 cells was determined by colocalizing PGRMC1 with β-tubulin (Fig. 5A). At metaphase, PGRMC1 localized to the spindle apparatus, as indicated by its colocalization with β-tubulin (Fig. 6A, top row). PGRMC1 was also present at the mitotic spindle poles, suggesting that it localizes to the centrosome. The centrosome localization was confirmed, because PGRMC1 colocalized with γ-tubulin, a specific marker of centrosomes [25]. PGRMC1 also localized to the midzone and the midbody (Fig. 5B) at anaphase/telophase and cytokinesis, respectively

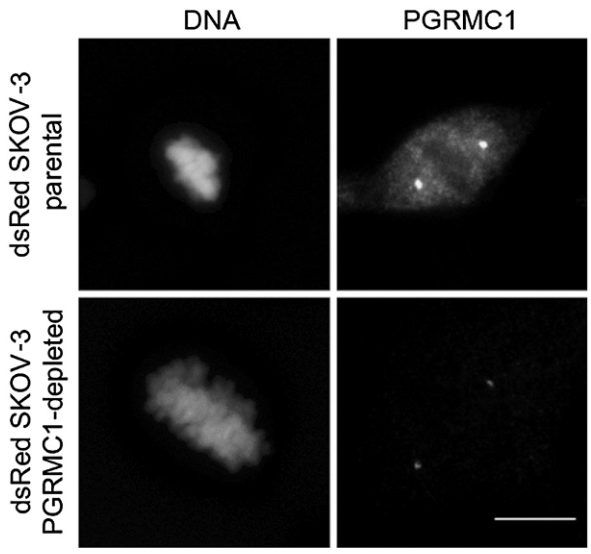

FIG. 6. Representative images showing immunodetection of PGRMC1 expression by immunofluorescence analysis in parental and PGRMC1-depleted dsRed SKOV-3 cells. Bar = 10 μm.

(Fig. 5B). When the effect of P4 treatment on PGRMC1 localization to the spindle apparatus was assessed, no differences were observed between treated and control groups (not shown).

In addition, immunofluorescence analysis confirmed and expanded Western blot analysis (Fig. 4A) by showing a marked reduction of PGRMC1 immunostaining in metaphase PGRMC1-depleted dsRed SKOV-3 (Fig. 6). In particular, the FI of PGRMC1 in the spindle area was reduced by 63% ($P < 0.05$) compared with the parental dsRed SKOV-3 cells (mean ± SEM FI values were calculated on a total of 22 and 28 cells, respectively, and were 39.25 ± 20.04 for PGRMC1-depleted dsRed SKOV-3 cells, and 106.56 ± 27.07 for parental dsRed SKOV-3 cells).

Because colocalization data are not indicative of a physical association between PGRMC1 and β-tubulin or γ-tubulin, an in situ PLA was used to determine whether PGRMC1 directly interacts with either β-tubulin or γ-tubulin in mitotic cells. To confirm the efficiency of this technique, the interaction between α-tubulin and β-tubulin, which are known to form a heterodimer during microtubule polymerization [26], was assessed. As expected, immunofluorescent studies confirmed the colocalization of α-tubulin and β-tubulin in the mitotic spindle (Fig. 7A, top row), and the PLA detected a direct interaction (Fig. 7A, middle row). Negative controls were carried out by omitting one of the primary tubulin antibodies and did not reveal any signal (Fig. 7A, bottom row). As shown in Figure 7B, upper row, the PLA also demonstrated a clear interaction between PGRMC1 and β-tubulin. On the contrary, a direct interaction between PGRMC1 and γ-tubulin was not detected by PLA (Fig. 7B, lower row), even through these two proteins colocalized (Fig. 5A). This observation thereby illustrates the specificity of the PLA. Finally, P4 treatment did not affect the amount of PGRMC1-β-tubulin interaction, as judged by the intensity of the PLA signal (data not shown).

DISCUSSION

Previous work has shown that P4 inhibits mitosis of rat granulosa cells, human granulosa/luteal cells [7], and SIGCs [10]. Progesterone has also been shown to have a dose-dependent effect on proliferation of ovarian cancer cells, stimulating proliferation at nanomolar concentrations but inhibiting growth micromolar concentrations [13, 14]. The present studies expand these observations by demonstrating that a component of P4's antimitotic action involves its ability to increase the percentage of mitotic figures. This suggests that P4 regulates the rate at which cells progress through the M phase of the cell cycle.

Mitotic progression is a dynamic process that primarily depends on the formation and function of the mitotic spindle. The key structural components of the mitotic spindle are the microtubules, which are composed of polymers of α-tubulin and β-tubulin (reviewed in Desai and Mitchison [26]). The microtubules dynamically assemble and disassemble to ''search out'' and bind to the condensed chromosomes. Once in contact with chromosomes, the microtubules promote chromosomal segregation into two daughter cells (reviewed in Gadde and Heald [27]).

In previous studies, P4's effect on microtubule assembly has been tested by monitoring the in vitro assembly (polymerization) of purified tubulin [28–30]. These studies showed that although P4 binds the microtubule-associated protein 2 (MAP2), micromolar doses of P4 do not stimulate microtubule assembly. In contrast, P4 antagonizes pregnenolone's ability to bind MAP2 and to stimulate MAP2-dependent microtubule assembly [28–30]. Although P4 failed to affect the assembly of purified tubulin in vitro, this does not necessarily mean that P4 does not influence microtubule function. This is because this in vitro system has two major limitations. First, it cannot assess the stability of the microtubules, and second, it does not reflect the complexities involved in microtubule stability in a living cell [27, 31].

The present study used an intact cell system in which the stability of the mitotic spindle can be assessed in a quantitative manner. Using this approach, our studies are the first to demonstrate that P4 increases spindle microtubule stability as judged by its ability to inhibit the disassembly of the mitotic spindle in response to cooling. The P4-induced stability of the microtubules could impede the ability of the microtubules to establish an appropriate contact with the chromosomes and/or interfere with microtubule-dependent segregation of the metaphase chromosomes. Either of these possibilities could account in part for P4's ability to increase the percentage of mitotic figures. This concept is consistent with the experimental evidence that demonstrates that P4 1) facilitates chromosome instability, which leads to aberrant chromosomal segregation (i.e., aneuploidy) in p53 null mammary epithelial cells [32, 33], and 2) promotes abnormal mitoses in rat liver [34].

How P4 promotes stability of the spindle microtubules is not known. Insight into the mechanism of P4's action is provided by the observation that PGRMC1 localizes to the mitotic spindle apparatus, where it not only colocalizes with but also physically interacts with β-tubulin, as revealed by PLA. A comparison of the effects of P4 and PGRMC1 depletion reveals that both of these treatments increase microtubule stability and suppress cell proliferation. The fact that depleting PGRMC1 from the mitotic spindle has the same effect as P4 treatment suggests that P4 acts to prevent PGRMC1 from exerting its function on the mitotic spindle, thus affecting the spindle stability, and ultimately the mitotic progression.

Surprisingly, P4 treatment altered neither PGRMC1's localization to the spindle apparatus, nor its direct interaction with β-tubulin. However, P4 would not necessarily have to remove PGRMC1 from the microtubules in order to affect its stability. For example, P4 could alter PGRMC1's action by changing its phosphorylation status, because it is known that

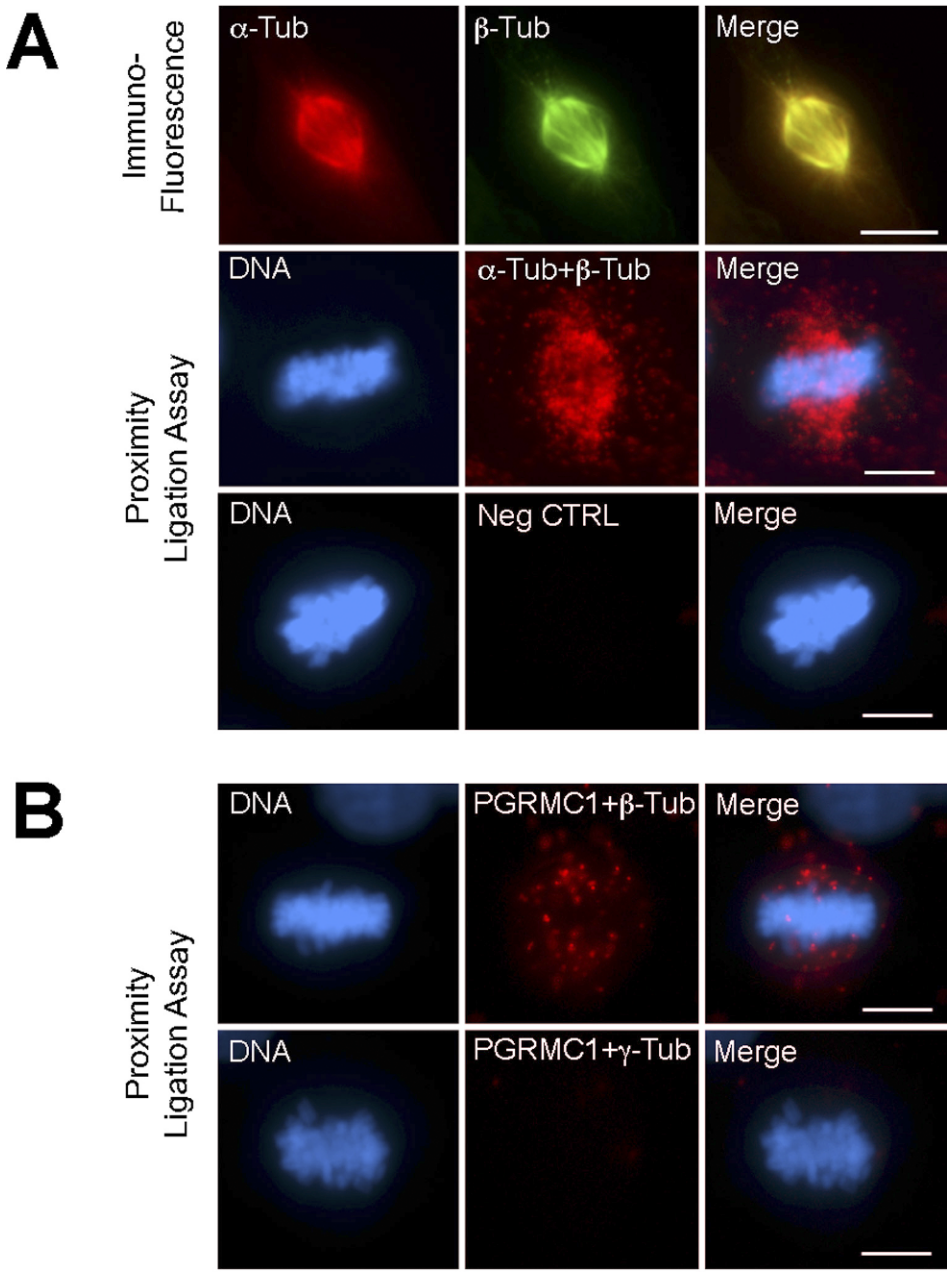

FIG. 7. Representative images showing the interaction between α-tubulin (α-Tub) and β-tubulin (β-Tub; **A**) and PGRMC1 and either β-tubulin or γ-tubulin (γ-Tub; **B**) in mitotic SKOV-3 cells, as revealed by in situ PLA. The presence of red fluorescent dots in the PLA assay indicates that two proteins are in close proximity (i.e., interacting). DNA is counterstained with 4′,6′-diamidino-2-phenylindole (DAPI; blue). In **A**, the lowest row is an example of a negative control obtained by omitting the anti-α-tubulin antibody. As a comparison of a standard immunofluorescent staining and the PLA assay, in **A** (top row) is shown the immunofluorescent staining of α-tubulin and β-tubulin (red and green, respectively). Bar = 10 μm.

PGRMC1 on the human mitotic spindle is phosphorylated at serine 180 [18]. It is possible, then, that P4 binding to PGRMC1 could promote its phosphorylation by one of the numerous kinases that are present at specific sites along the mitotic spindle [35, 36]. This, in turn, could alter spindle microtubule stability, and ultimately control the rate of mitotic progression. Support for this hypothesis comes from the observation that PGRMC1 colocalizes with active-form Aurora B kinase during oocyte meiosis [37]. Therefore, in future studies, it will be important to determine whether PGRMC1 localization and/or interaction with β-tubulin are dependent on its phosphorylation status, and whether this is regulated by P4.

Finally, it is important to appreciate that P4-PGRMC1 interaction does not always result in the suppression of mitosis. In neural progenitor cells, P4 stimulates ERK activity, and ultimately cell proliferation [38]. Moreover, P4's ability to induce ERK activity and promote entry into the cell cycle is dependent on PGRMC1 [38]. Conversely, in SIGCs, P4 suppresses ERK activity [39] and inhibits mitosis (the present study and Peluso et al. [10]). The reason for the different responses is unclear but may be related to the expression of various progestin receptors within a given cell type. Interestingly, progestin and adipoQ receptors (PAQRs) increase the activity of ERK in response to P4 treatment (Karteris et al. [40] and Zhu et al. [41]; reviewed in Peluso [42]). It is possible that the neural progenitor cells express PAQRs, whereas SIGCs may not express these receptors. Thus, the putative tissue-specific expression of PGRMC1 and PAQRs, as well as the nuclear progesterone receptors A and B, could account for differing responses to P4 that are observed in neural progenitor cells compared with SIGC and SKOV-3 cells.

In summary, the results presented in this study suggest that in SIGCs and SKOV-3 cells, micromolar doses of P4 slow cell proliferation and delay mitotic progression, possibly through the regulation of a microtubule-dependent process. Progesterone's action appears to be mediated in part by PGRMC1, suggesting a crucial role for PGRMC1 during ovarian cell mitosis. The precise relationship between P4 and PGRMC1 is

not known, but P4-PGRMC1 interactions could regulate the stability of the microtubules, and thereby govern the rate of mitosis.

ACKNOWLEDGMENTS

The authors would like to thank Dr. Robert Burghardt for providing the SIGCs and Xiufang Liu for her excellent technical assistance.

REFERENCES

1. Mahesh VB, Muldoon TG. Integration of the effects of estradiol and progesterone in the modulation of gonadotropin secretion. J Steroid Biochem 1987; 27:665–675.
2. Muldoon TG, Mahesh VB. Receptor-weighted mechanistic approach to analysis of the actions of estrogen and progesterone on gonadotropin secretion. Adv Exp Med Biol 1987; 219:47–64.
3. Kurita T, Lee K, Saunders PT, Cooke PS, Taylor JA, Lubahn DB, Zhao C, Makela S, Gustafsson JA, Dahiya R, Cunha GR. Regulation of progesterone receptors and decidualization in uterine stroma of the estrogen receptor-alpha knockout mouse. Biol Reprod 2001; 64:272–283.
4. Spencer TE, Johnson GA, Burghardt RC, Bazer FW. Progesterone and placental hormone actions on the uterus: insights from domestic animals. Biol Reprod 2004; 71:2–10.
5. Peluso JJ. Multiplicity of progesterone's actions and receptors in the mammalian ovary. Biol Reprod 2006; 75:2–8.
6. Gellersen B, Fernandes MS, Brosens JJ. Non-genomic progesterone actions in female reproduction. Hum Reprod Update 2009; 15:119–138.
7. Chaffkin LM, Luciano AA, Peluso JJ. The role of progesterone in regulating human granulosa cell proliferation and differentiation in vitro. J Clin Endocrinol Metab 1993; 76:696–700.
8. diZerega GS, Hodgen GD. The interovarian progesterone gradient: a spatial and temporal regulator of folliculogenesis in the primate ovarian cycle. J Clin Endocrinol Metab 1982; 54:495–499.
9. Luciano AM, Peluso JJ. Effect of in vivo gonadotropin treatment on the ability of progesterone, estrogen, and cyclic adenosine 5′-monophosphate to inhibit insulin-dependent granulosa cell mitosis in vitro. Biol Reprod 1995; 53:664–669.
10. Peluso JJ, Fernandez G, Pappalardo A, White BA. Membrane-initiated events account for progesterone's ability to regulate intracellular free calcium levels and inhibit rat granulosa cell mitosis. Biol Reprod 2002; 67: 379–385.
11. Peluso JJ, Pappalardo A. Progesterone mediates its anti-mitogenic and anti-apoptotic actions in rat granulosa cells through a progesterone-binding protein with gamma aminobutyric acidA receptor-like features. Biol Reprod 1998; 58:1131–1137.
12. Stouffer RL. Progesterone as a mediator of gonadotrophin action in the corpus luteum: beyond steroidogenesis. Hum Reprod Update 2003; 9:99–117.
13. Ho SM. Estrogen, progesterone and epithelial ovarian cancer. Reprod Biol Endocrinol 2003; 1:73.
14. Syed V, Ulinski G, Mok SC, Yiu GK, Ho SM. Expression of gonadotropin receptor and growth responses to key reproductive hormones in normal and malignant human ovarian surface epithelial cells. Cancer Res 2001; 61:6768–6776.
15. Fujii T, Hoover DJ, Channing CP. Changes in inhibin activity, and progesterone, oestrogen and androstenedione concentrations, in rat follicular fluid throughout the oestrous cycle. J Reprod Fertil 1983; 69: 307–314.
16. Peluso JJ, Gawkowska A, Liu X, Shioda T, Pru JK. Progesterone receptor membrane component-1 regulates the development and Cisplatin sensitivity of human ovarian tumors in athymic nude mice. Endocrinology 2009; 150:4846–4854.
17. Ahmed IS, Rohe HJ, Twist KE, Mattingly MN, Craven RJ. Progesterone receptor membrane component 1 (Pgrmc1): a heme-1 domain protein that promotes tumorigenesis and is inhibited by a small molecule. J Pharmacol Exp Ther 2010; 333:564–573.
18. Nousiainen M, Sillje HH, Sauer G, Nigg EA, Korner R. Phosphoproteome analysis of the human mitotic spindle. Proc Natl Acad Sci U S A 2006; 103:5391–5396.
19. Stein LS, Stoica G, Tilley R, Burghardt RC. Rat ovarian granulosa cell culture: a model system for the study of cell-cell communication during multistep transformation. Cancer Res 1991; 51:696–706.
20. Peluso JJ, Liu X, Gawkowska A, Lodde V, Wu CA. Progesterone inhibits apoptosis in part by PGRMC1-regulated gene expression. Mol Cell Endocrinol 2010; 320:153–161.
21. Peluso JJ, Pappalardo A, Fernandez G. Basic fibroblast growth factor maintains calcium homeostasis and granulosa cell viability by stimulating calcium efflux via a PKC delta-dependent pathway. Endocrinology 2001; 142:4203–4211.
22. Deshayes S, Morris M, Heitz F, Divita G. Delivery of proteins and nucleic acids using a non-covalent peptide-based strategy. Adv Drug Deliv Rev 2008; 60:537–547.
23. Appierto V, Tiberio P, Cavadini E, Casalini P, Cappelletti G, Formelli F. Antimitotic effect of the retinoid 4-oxo-fenretinide through inhibition of tubulin polymerization: a novel mechanism of retinoid growth-inhibitory activity. Mol Cancer Ther 2009; 8:3360–3368.
24. Wu G, Lin YT, Wei R, Chen Y, Shan Z, Lee WH. Hice1, a novel microtubule-associated protein required for maintenance of spindle integrity and chromosomal stability in human cells. Mol Cell Biol 2008; 28:3652–3662.
25. Pereira G, Schiebel E. Centrosome-microtubule nucleation. J Cell Sci 1997; 110(pt 3):295–300.
26. Desai A, Mitchison TJ. Microtubule polymerization dynamics. Annu Rev Cell Dev Biol 1997; 13:83–117.
27. Gadde S, Heald R. Mechanisms and molecules of the mitotic spindle. Curr Biol 2004; 14:R797–R805.
28. Fontaine-Lenoir V, Chambraud B, Fellous A, David S, Duchossoy Y, Baulieu EE, Robel P. Microtubule-associated protein 2 (MAP2) is a neurosteroid receptor. Proc Natl Acad Sci U S A 2006; 103:4711–4716.
29. Mizota K, Ueda H. N-terminus of MAP2C as a neurosteroid-binding site. Neuroreport 2008; 19:1529–1533.
30. Murakami K, Fellous A, Baulieu EE, Robel P. Pregnenolone binds to microtubule-associated protein 2 and stimulates microtubule assembly. Proc Natl Acad Sci U S A 2000; 97:3579–3584.
31. Holmfeldt P, Sellin ME, Gullberg M. Predominant regulators of tubulin monomer-polymer partitioning and their implication for cell polarization. Cell Mol Life Sci 2009; 66:3263–3276.
32. Goepfert TM, McCarthy M, Kittrell FS, Stephens C, Ullrich RL, Brinkley BR, Medina D. Progesterone facilitates chromosome instability (aneuploidy) in p53 null normal mammary epithelial cells. FASEB J 2000; 14: 2221–2229.
33. Pati D, Haddad BR, Haegele A, Thompson H, Kittrell FS, Shepard A, Montagna C, Zhang N, Ge G, Otta SK, McCarthy M, Ullrich RL, et al. Hormone-induced chromosomal instability in p53-null mammary epithelium. Cancer Res 2004; 64:5608–5616.
34. Boada LD, Zumbado M, del Rio I, Blanco A, Torres S, Monterde JG, Afonso JL, Cabrera JJ, Diaz-Chico BN. Steroid hormone progesterone induces cell proliferation and abnormal mitotic processes in rat liver. Arch Toxicol 2002; 75:707–716.
35. Ruchaud S, Carmena M, Earnshaw WC. Chromosomal passengers: conducting cell division. Nat Rev Mol Cell Biol 2007; 8:798–812.
36. Lukasiewicz KB, Lingle WL. Aurora A, centrosome structure, and the centrosome cycle. Environ Mol Mutagen 2009; 50:602–619.
37. Luciano AM, Lodde V, Franciosi F, Ceciliani F, Peluso JJ. Progesterone receptor membrane component-1 expression and putative function in bovine oocyte maturation, fertilization and early embryonic development. Reproduction 2010; 140:663–672.
38. Liu L, Wang J, Zhao L, Nilsen J, McClure K, Wong K, Brinton RD. Progesterone increases rat neural progenitor cell cycle gene expression and proliferation via extracellularly regulated kinase and progesterone receptor membrane components 1 and 2. Endocrinology 2009; 150:3186–3196.
39. Peluso JJ, Bremner T, Fernandez G, Pappalardo A, White BA. Expression pattern and role of a 60-kilodalton progesterone binding protein in regulating granulosa cell apoptosis: involvement of the mitogen-activated protein kinase cascade. Biol Reprod 2003; 68:122–128.
40. Karteris E, Zervou S, Pang Y, Dong J, Hillhouse EW, Randeva HS, Thomas P. Progesterone signaling in human myometrium through two novel membrane G protein-coupled receptors: potential role in functional progesterone withdrawal at term. Mol Endocrinol 2006; 20:1519–1534.
41. Zhu Y, Bond J, Thomas P. Identification, classification, and partial characterization of genes in humans and other vertebrates homologous to a fish membrane progestin receptor. Proc Natl Acad Sci U S A 2003; 100: 2237–2242.
42. Peluso JJ. Non-genomic actions of progesterone in the normal and neoplastic mammalian ovary. Semin Reprod Med 2007; 25:198–207.